Polymer 53 (2012) 3220–3229

Contents lists available at SciVerse ScienceDirect

Polymer

journal homepage: www.elsevier.com/locate/polymer

Particle formation and characteristics of Celecoxib-loaded poly(lactic-co-glycolic acid) microparticles prepared in different solvents using electrospraying

Adam Bohr [a,b,c], Mingshi Yang [b], Stefanía Baldursdóttir [b], Jakob Kristensen [c], Mark Dyas [c], Eleanor Stride [a,d], Mohan Edirisinghe [a,*]

[a] Department of Mechanical Engineering, University College London, Torrington Place, London WC1E 7JE, UK
[b] Department of Pharmaceutics and Analytical Chemistry, The Faculty of Pharmaceutical Sciences, University of Copenhagen, Universitetsparken 2, DK-2100 Copenhagen, Denmark
[c] Veloxis Pharmaceuticals A/S, Kogle Allé 4, DK-2970 Hørsholm, Denmark
[d] Institute of Biomedical Engineering, Department of Engineering Science, University of Oxford, Old Road Campus Research Building, Headington OX3 7DQ, UK

ARTICLE INFO

Article history:
Received 13 February 2012
Received in revised form
20 April 2012
Accepted 3 May 2012
Available online 11 May 2012

Keywords:
Particle formation
Electrospraying
Drug release

ABSTRACT

Microparticles were fabricated for pharmaceutical purposes using electrospraying with the aim to determine the effect of the solvent(s) used. Particles of poly(lactic-co-glycolic acid) (PLGA) and the drug Celecoxib were prepared from acetone, acetonitrile and acetone:methanol with different polymer and drug concentrations. The solvent power, evaporation rate and electrical conductivity of the solvents all had a significant effect on the particle formation process as well as the particle characteristics and drug release profile. Particles were near-spherical and between 2 and 7 μm in diameter with smooth or corrugated surfaces. The drug release rate was mainly dependent on particle size, with larger particles showing slower release. The solvent in which PLGA was poorly soluble resulted in small grainy particles that disintegrated instantaneously with full drug release. It may be concluded that the selection of an appropriate solvent may be a useful way to control particle characteristics and drug release profiles when using electrospraying.

1. Introduction

The entrapment of drugs in polymer microparticles continues to be of interest for new drug formulation strategies. Compared with conventional drug formulations, microparticles with drug entrapped in a polymer matrix allow better control of delivery particularly for large molecules such as proteins and nucleic acids as well as small molecule drugs with low aqueous solubility [1–3]. The matrix protects, stabilizes, and increases the efficiency of the drug and the release kinetics can be controlled by manipulating the physical and chemical properties of the polymer surrounding the drug molecules as well as the structural features of the microparticles [4,5]. Several types of polymers have been used for drug encapsulation and of these poly(lactic-co-glycolic acid) (PLGA) is among the most widely studied due to its biodegradability and its compatibility with many different molecules. Furthermore, PLGA is FDA approved and is amorphous when containing glycolic acid in the range of 25–70% [6]. Yet, despite the extensive studies on microparticles for controlled release using PLGA systems, the mechanism of drug release from PLGA microparticles is not fully understood. This is partly due to the complexity of the processes and the interactions present in such a system but also because of the lack of understanding on the relationship between particle characteristics and drug release [7].

There are several existing technologies for producing microparticles for drug delivery purposes with the most popular being emulsion-based techniques and spray drying. With emulsion-based techniques, drug molecules are mixed into a polymer solution and emulsified in a water or an oil phase to form micro droplets and then dried via solvent removal to form dry particles. This method however has several disadvantages such as the time consuming process of removing the solvents, the poor drug loading capacity of the particles and the numerous steps involved in the processing. It is further limited by hygroscopic properties of the drug, requires additives such as surfactants and typically results in a broad particle size distribution [3,8,9]. Spray drying is another widely applied pharmaceutical technology for producing microparticles both at laboratory and commercial scale. Here the feed solution containing polymer and/or drug is atomized at elevated temperatures in a chamber under a constant air flow and dried microparticles are collected. Although spray drying is a simple and attractive particle preparation method it has the limitation of

* Corresponding author. Tel.: +44 20 76793942; fax: +44 20 73880180.
E-mail address: m.edirisinghe@ucl.ac.uk (M. Edirisinghe).

0032-3861/$ – see front matter © 2012 Elsevier Ltd. All rights reserved.
doi:10.1016/j.polymer.2012.05.002

producing particles with a relatively broad size distribution, may often suffer from agglomeration of particles and the elevated temperatures involved can lead to instability of thermosensitive molecules [10–12].

Several studies have indicated that a monodisperse particle size distribution provides better control over drug release and therefore improves therapeutic effect [13,14]. Particle morphology has also been demonstrated to influence several aspects of drug delivery mechanisms and engineering particles with different morphologies and surface characteristics is thus relevant. It has been shown by some researchers that phagocytic internalization of polymeric based particles is dependent on the shape of the particles [15]. Also, the drug release kinetics and targeting abilities of microparticles have been observed to be influenced by the particle surface chemistry, morphology and curvature [16,17]. It is therefore evident that it is important to control homogeneity in terms of both size and morphology of the particles.

There is an increased interest in the fabrication of polymeric microparticles using electrospraying with numerous studies in recent years on electrosprayed particles for pharmaceutical purposes [13,18,19]. Electrospraying utilizes electrostatic forces to control the break up of a liquid flow to form droplets and hence microparticles. It is both simple and inexpensive and largely overcomes the limitations of aforementioned techniques, producing monodisperse microparticles with control over their size and morphology without the need of surfactants or elevated temperatures [20,21]. Yet, electrospraying is a complex process in terms of controlling the process of particle formation as the underlying mechanisms are influenced by many variables including: flow rate, electric field strength, solution properties and external conditions [21,22]. Many of these variables have an interdependent influence on the resulting particle properties and drug release profile, and it is thus challenging to fully optimize the final output. Typically, in the studies applying electrospraying, an emphasis is placed on the final particle product and the characterization thereof. Meanwhile, more detailed understanding of the particle formation is not fully explained although some findings have been reported [23–25]. It is critical for the optimization of electrospraying as a processing technique to have some insight into the mechanisms that influence the process of particle formation and this is the object of this study.

Specifically, we investigated the formation of drug-loaded microparticles with a focus on the solvents used, to examine how this factor influences the final particle characteristics and release of the drug from the particles. For this purpose a small molecule drug, Celecoxib (CEL), was used as the model drug. CEL is a non-steroidal, anti-inflammatory drug with a poor aqueous solubility [26]. PLGA (50:50, $M_w = 33000$) was used as the polymeric carrier. Further, three solvent systems were investigated, i.e. acetone and acetonitrile, which are good solvents for both CEL and PLGA, and a binary solvent consisting of acetone and methanol, in which methanol is a poor solvent for PLGA. The objectives of this study were to investigate the role of these different solvents in the process of particle formation via electrospraying by examining the particle characteristics and release behavior of these CEL-loaded PLGA microparticles.

2. Experimental

2.1. Materials

CEL crystalline powder was acquired from Dr. Reddy, Hyderabad, India ($M_w = 381.38$). Poly(D,L-lactide-co-glycolide (PLGA; 50:50 Resomer RG503H, $M_w = 33000$) was purchased from Boehringer Ingelheim (Ingelheim, Germany). Acetone (ACE, 99.9% HPLC grade), methanol (MeOH, 99.9% HPLC grade) and acetonitrile (ACN, 99.9% HPLC grade) were purchased from Sigma Aldrich (Poole, UK). Ultrapure water (SG Water Purification System, Barsbuttel, Germany) was used for all the experiments. Phosphate Buffered Saline (PBS, 0.01 M, pH 6.8) was made from sodium phosphate monobasic and sodium hydroxide purchased from Sigma Aldrich (Poole, UK), and Sodium Lauryl Sulphate (SLS) was purchased from Fagron (Waregem, Belgium). All other chemicals and solvents were of analytical grade and used without further purification.

2.2. Characterization of spraying solutions

The properties of the solvents used, are shown in Table 1. The values for density, boiling point, evaporation rate, dielectric constant were obtained from literature [27]. The values for electrical conductivity of the solvents and the spraying solutions were measured using a multimeter (InLab, Mettler Toledo). The viscosity of the solvents and spraying solutions were determined using an Ubbelohde viscometer (Cannon Instruments) at 25 °C in a water bath. The intrinsic viscosity ($[\eta]$) of PLGA in the different solvents was determined by extrapolation of the values for specific viscosity η_{sp} as the polymer concentration, c, went to zero using equation (1) [28]. Seven different concentrations were measured for each PLGA-solvent combination. Further, the Martin constant (K_m) was calculated for the solutions with 5% polymer concentration by using equation (2), the Martin equation [29]. Also, the overlap concentration (c^*) for PLGA in the different solvents was calculated using equation (3) [30].

$$[\eta] = \lim_{c\to 0}\left(\frac{\eta_{sp}}{c}\right) \tag{1}$$

$$\frac{\eta_{sp}}{[\eta]c} = \exp(K_m[\eta]c) \tag{2}$$

$$c^* = \frac{1}{[\eta]} \tag{3}$$

2.3. Preparation of microparticles

Microparticles consisting of PLGA and CEL were fabricated using a single-nozzle electrospraying setup where a thin jet is dispersed into small droplets that dry into particles (see Fig. 1). The solutions with different solute concentration (3, 5 and 7 wt.%) and different drug loading (10 and 30 wt.%) were prepared by dissolving appropriate amounts of CEL and PLGA in different solvents (i.e. acetone, acetonitrile or acetone:methanol (75:25 M ratio). The electrospraying setup applied consisted of a high voltage power source (Glassman Europe Ltd, Tadley, UK), a high precision mechanical syringe pump (PHD 4400, Harvard Apparatus, Edenbridge, UK) and a custom-built concentric stainless steel nozzle with outer and inner diameters of 2.34 mm and 1.77 mm,

Table 1
Physical properties of solvents used to fabricate microparticles.

Physical properties	Acetone	Acetonitrile	Methanol
Density at 25 °C (kg m^{-3})	*790*	*782*	*792*
Viscosity (mPa s) at 25 °C	0.30	0.35	0.57
Boiling point (°C)	*56.0*	*82*	*64.0*
Evaporation rate (BuAc = 1)[a]	*5.6*	*2.0*	*4.1*
Electrical conductivity (μS/m)	6	23	50
Solubility of PLGA	Soluble	Soluble	Insoluble
Solubility of CEL	Soluble	Soluble	Soluble

Values in *italic* are from the solvent handbook.
[a] Relative to the evaporation rate of Butyl Acetate.

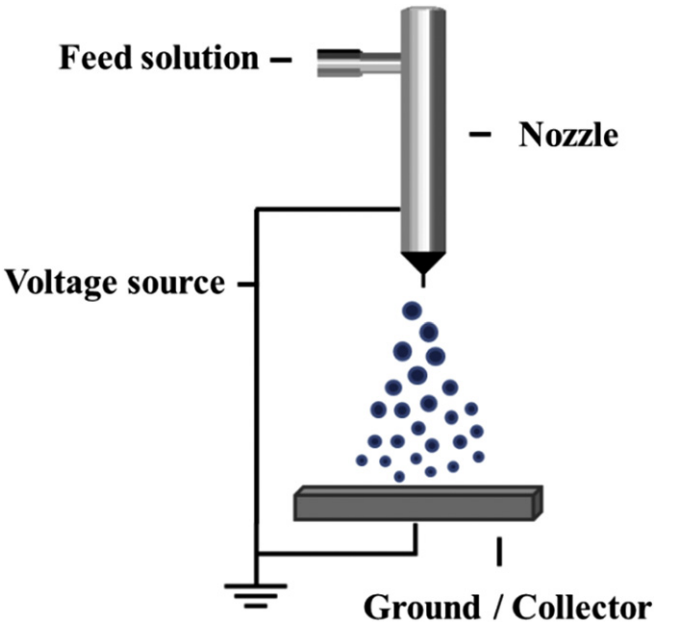

Fig. 1. Schematic diagram of electrospraying setup.

respectively. All solutions were electrosprayed with an applied electrical potential difference of between 10 and 13 kV with the positive electrode attached to the tip of the nozzle and the negative electrode to the collector. The particles produced from electrospraying were collected at a distance of 70 mm from the nozzle either onto a microscope slide containing distilled water or onto a sheet of aluminum foil. The particle samples were left to dry completely in a desiccator under vacuum. A video camera with an in-built magnifying lens (Leica S6D JVC-color) was used to observe the nozzle tip at all times during the preparation of the microparticles.

2.4. Particle size and morphology

The morphology and size of the microparticles were characterized using a scanning electron microscope (SEM) (JEOL JSM-6301F and Hitachi VP-SEM S-3400N). The microparticles were sprayed on to glass slides as a thin layer and were sputter-coated with gold, mounted on metallic studs and viewed at an accelerating voltage of 3 kV (for JEOL JSM-6301F) or 10 kV (for Hitachi VP-SEM S-3400N). The SEM images were used to calculate the mean diameter and polydispersivity index for each of the microparticle samples studied. Between 200 and 300 microparticles were measured from different sites of the sample, using the image analysis software ImageJ (NIH).

2.5. Drug loading and entrapment efficiency

The drug loading and entrapment efficiency (EE) of CEL in the microparticles was measured by determining the total amount of CEL in the microparticle samples. In brief, 15–20 mg samples of the microparticles were dissolved in 10 ml acetonitrile and agitated for 1 h under sealed conditions. Then, 1 ml of the solution was aliquoted and diluted 1:10 in a solution of acetonitrile:water (9:91 M ratio) and mixed. The drug content in this mixed solution was then analyzed by using reverse phase HPLC, UVD340U (Dionex, Germany) equipped with a Kromasil 126 column (Kromasil, Sweden). The mobile phase consisted of an acetonitrile:-water (52:48 M ratio) solution and was used at a flow rate of 0.5 ml min^{-1} and a 10 μl injection volume was measured over a run time of 15 min at a wavelength of 230 nm. A calibration curve was obtained from CEL solutions in the range 0.5–50 μg/ml and a good linear correlation was found over the entire range. The drug entrapment efficiency was calculated using equations (4) and (5):

$$\text{Drug loading}(\%) = (M_{\text{actual}}/\text{weighed amount of composite particles})100 \quad (4)$$

$$\text{Entrapment efficiency}(\%) = (M_{\text{actual}}/M_{\text{theoretical}})100 \quad (5)$$

2.6. Drug release study

Drug release studies were performed on a Sotax AT7 dissolution station (Sotax, Switzerland) equipped with a USP II paddle apparatus and 1 L glass vessels. Samples of 5 mL were drawn through 2.7 μm glass microfiber filters (Whatman, England) using an autosampler, Biolab/Gilson GX-271 (Biolab, UK). Microparticle samples of 15–20 mg were placed in vessels containing 500 ml dissolution media and the dissolution apparatus was run at a paddle rotation of 50 rpm and a temperature of 37 °C. The dissolution media consisted of PBS (0.01 M, pH 6.8) + 1.5% SLS and sink conditions applied, the volume of dissolution media was at least 3 times greater than the saturation point of CEL. Samples were drawn at predetermined time intervals up to 20 h and subsequently transferred to HPLC vials. The HPLC measurements were run as described for drug entrapment efficiency and release data were analyzed using the software Chromeleon 6.8 (Dionex, Germany).

Selected drug release data were curve fitted using the Higuchi release model, a simplified model based on modifications of Fick law of diffusion, with the following equation [31]:

$$Q = k_h t^{1/2}$$

where Q is the amount of drug released at the time, t, and k_h is the Higuchi dissolution constant. The Higuchi model was modified by using a level 2 polynomial regression instead of a linear regression.

3. Results

3.1. Characterization of solvent systems and polymer solutions

Two solvent properties, i.e. boiling point and solvent power (the ability of a solvent to dissolve solutes, in this case PLGA and CEL) were examined to investigate effects of the solvents on the characteristics of microparticles produced from the electrospraying process. Solvents for preparation of the microparticles were selected based on the criteria that both CEL and PLGA needed to be soluble in them. Further, the solvents needed to be volatile enough to result in dry particles upon collection. Following these criteria the solvents ACN and ACE were selected, which have similar densities but significantly different boiling points (see Table 1). In addition, a binary solvent of ACE and MeOH was also used with MeOH being a poor solvent to PLGA.

The values presented in Table 1 demonstrate that the solvents, apart from having different boiling points and evaporation rates also have different electrical conductivities and viscosities. The values showed that ACE was the least conductive and least viscous of the three and MeOH was the most conductive and most viscous. Both viscosity and electrical conductivity are known to play an important role in electrospraying and hence controlling the properties of the microparticles obtained, most notably an increase in conductivity and decrease and viscosity resulting in decrease of particle size [32,33]. The measurements of electrical conductivity in

Table 2
Electrical conductivity of solutions containing CEL or PLGA.

Solution	5% CEL in ACE	5% CEL in ACN	5%CEL in ACE/MeOH	5% PLGA in ACE	5% PLGA in ACN	5% PLGA in ACE/MeOH
Electrical conductivity (μS/m)	101	106	109	23	40	32

solvents containing either 5%wt CEL or PLGA showed that the contribution by CEL to the conductivity is larger than for PLGA at the same concentration (Table 2).

Measurement of the intrinsic viscosity was performed to determine the solubility and behavior mainly of PLGA in the different solvents. The contribution of CEL to the viscosity is insignificant compared with PLGA due to its low molecular weight and moreover only PLGA is relevant in the context of polymer entanglement during particle formation. The intrinsic viscosity refers to the capability of a specific polymer to enhance the viscosity of the solvent in which it is dissolved. This depends partly on the molecular weight of the polymer and the polymer–solvent compatibility [28]. The intrinsic viscosity of PLGA in the solvents was between 0.127 and 0.276 dL/g (see Table 3) indicating a relatively low fluid dynamic volume of the polymer chains in all the measured solvents. In ACE, PLGA showed the highest intrinsic viscosity and in ACE/MeOH it showed the lowest value demonstrating the compact conformation of the polymer chains in ACE/MeOH and a better solubility of the PLGA in ACE [34]. This is an important parameter that influences the process of microparticle formation as it correlated to the degree to which the polymer forms intra or inter-polymer chain entanglements in the solution and during drying. Polymer entanglements become more significant as the polymer concentration increases and is believed to take place at some point in particle formation during electrospraying [23]. The Martin constant (K_m) is similarly used to indicate the interactions between solutes and between solute and solvent, with a higher value indicating more polymer–polymer interaction. In this case ACE/MeOH showed the highest Martin constant and ACE showed the lowest Martin constant indicating a higher degree of interactions between PLGA and ACE, than for PLGA and ACE/MeOH [25]. The overlap concentration (c^*) indicates the transition concentration of polymer in a solvent at which the intermolecular interactions become important and transient networks are formed. In other words, this is the concentration at which the intra and inter-polymer chain entanglements begin to form [30]. It is observed that ACE has the lowest overlap concentration while ACE:MeOH has the highest overlap concentration. This means that PLGA chain entanglements begin to form at a lower concentration in ACE than in the two other solvents. Moreover, chain entanglements may already have begun to form for some solutions before the electrospraying process and may not yet have formed in other solutions.

Table 3
Intrinsic viscosity, Martin constant and overlap concentration of PLGA in different solvents.

Solvent	Acetone	Acetonitrile	Acetone:methanol (75:25)
Intrinsic viscosity (dL/g)	0.276, $R^2 = 0.981$	0.216, $R^2 = 0.978$	0.127, $R^2 = 0.997$
Martin constant (K_m)	0.480	0.629	1.297
Overlap concentration (c^*)	3.60	4.63	7.9

3.2. Particle morphology and size

To study the effect of different solvents on the formation of microparticles in the electrospraying process the size and morphology of the microparticles were examined as a function of solute concentration and drug loading (see Table 4). Representative SEM images from each of the microparticle samples are shown in Fig. 2A-L. The SEM images show that most of the generated microparticles had a near-spherical geometry with smooth, porous or grainy surfaces. The microparticles prepared with 7% solute concentration (Fig. 2E–H) generally exhibited less surface porosity compared with lower solute concentrations. For example samples 3S10A and 3S30A have a raisin-like morphology (Fig. 2A and B), those from sample 3S30N (Fig. 2D) are collapsed with large pores inside and those from sample 5S20M (Fig. 2K and L) consists of small grains (~100 nm in diameter) that are aggregated.

The diameter of the particles was found to range between 2 and 7 μm and the mean particle diameters from the different samples are listed in Table 4. Fig. 3 shows the particle diameters presented as a column chart with arrows indicating the influence of viscosity, electrical conductivity and solvent power. It can be seen that microparticles prepared with high solute concentration (high viscosity) and low drug loading (low electrical conductivity) are generally larger than those prepared at low solute concentration and high drug loading (See Fig. 3A). This trend is observed for both ACE and ACN, and furthermore particles prepared with ACE were slightly larger than those prepared with ACN in all cases. The particles prepared with the binary solvent of ACE and MeOH were significantly smaller than those prepared using ACE or ACN alone (see Fig. 3B).

3.3. Drug release studies

The drug entrapment efficiencies of the microparticle samples were found to be in the range of 88–99% with no correlation between the entrapment efficiency and the solvents used. Release of CEL from the microparticles was measured for each of the samples and release profiles are shown in Figs. 4–6. The microparticles all release between 88 and 98% of their drug content

Table 4
List of samples prepared. Solute conc. and polymer conc. are presented in % w/v and drug loading is presented in % w/w.

Sample code	Solute conc. (%)	Polymer conc. (%)	Drug loading (%)	Solvent	Particle diameter (μm)
3S10A	3	2.7	10	ACE	3.6 ± 0.4
3S30A	3	2.1	30	ACE	3.3 ± 0.4
3S10N	3	2.7	10	ACN	3.4 ± 0.3
3S30N	3	2.1	30	ACN	3.0 ± 0.3
7S10A	7	6.3	10	ACE	5.6 ± 0.9
7S30A	7	4.9	30	ACE	4.4 ± 0.5
7S10N	7	6.3	10	ACN	4.9 ± 0.4
7S30N	7	4.9	30	ACN	4.1 ± 0.4
5S20A	5	4.0	20	ACE	4.3 ± 0.5
5S20N	5	4.0	20	ACN	4.2 ± 0.3
5S20M	5	4.0	20	ACE/MeOH	2.9 ± 0.4

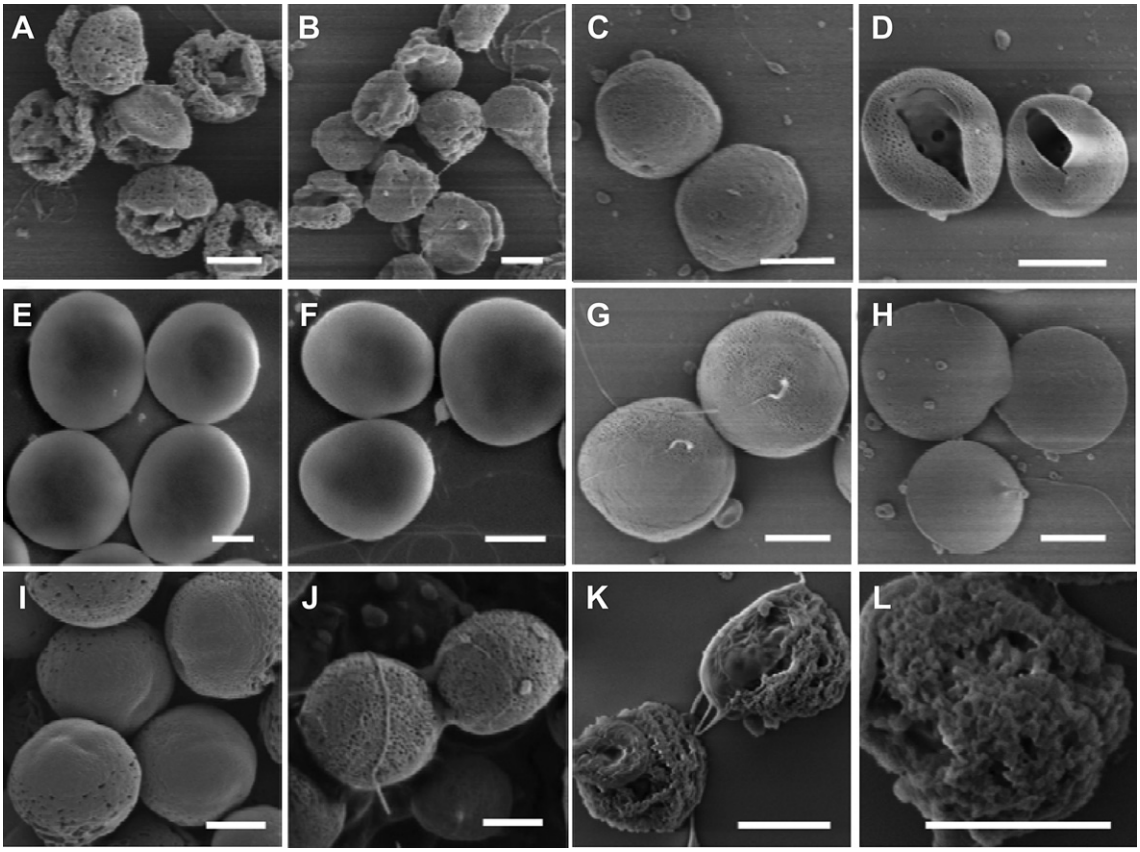

Fig. 2. SEM images of electrosprayed particle samples 3S10A (A), 3S30A (B), 3S10N (C), 3S30N (D), 7S10A (E), 7S30A (F), 7S10N (G), 7S30N (H), 5S20A (I), 5S20N (J), 5S20M (K) and 5S20M enlarged (L). The scale bar indicates 2 μm on all images.

within 20 h of exposure to the dissolution medium. Generally the particles produced with high solute concentration (Fig. 5) showed a slower release than those produced at a low solute concentration (Fig. 4), both for ACE and ACN. Also, the drug loading had a significant influence on release rate both at high and low solute concentration and for both ACE and ACN but particularly for ACN a clear difference was observed. When comparing the release profiles of particles prepared with ACE and ACN the trend observed is that those with ACE release their payload slightly slower than those with ACN, all except for samples 7S10A and 7S10N (Fig. 5). In Fig. 6 it is seen that samples 5S20A and 5S20N have relatively similar release curves while sample 5S20M releases much quicker. This indicates that adding a small amount of MeOH into the solution had a great effect on the drug release from the particles.

Fig. 7 shows selected release curves fitted with a modified version of the Higuchi model for diffusion dependent release as a function of the square root of time. All four curves were fitted with a level 2 polynomial regression and gave the *y*-intercepts −2.3, −3.2, −12.6, −10.0 and R^2 values 0.997, 0.998, 0.999, 0.995 for the samples 5S20N, 7S30A, 7S10A and 7S10N, respectively. It is observed that all curves in Fig. 7 follow their trend line very well. The Higuchi diffusion model was not compatible with the release curve of the other particle samples as they released their payload at a quicker rate.

Particles were scooped out of the dissolution chamber after completing drug release studies and they were examined using SEM to observe whether they remained structurally intact after most of the drug had been released from them. Particles from samples 5S20A and 5S20M were selected for this purpose to observe the largest differences between the samples. Fig. 8 shows that particles from sample 5S20A were still intact and spherical in shape after losing 20% of their dry weight but were smaller than before dissolution. On the other hand particles from sample 5S20M showed no preservation of structure and they seemed to have disintegrated during drug release and agglomerated.

4. Discussion

4.1. Particle formation process in electrospraying

CEL-loaded PLGA microparticles were produced from ACE, ACN and ACE:MeOH via electrospraying at different solute concentration and drug loading applying the same flow rate and collection distance. Although essentially a one-step process, particle formation in electrospraying takes place through several mechanisms which can be divided into four phases that take place continuously (see Fig. 9).

1. The solution breaks down into small electrically charged droplets that repel each other and disperse into a shower. The droplets are drawn downwards to the collection point under gravity and electrical forces and evaporation of the solvent occurs mainly from the surface of the droplets resulting in a progressive decrease in droplet diameter [35].
2. The electric charge of each droplet remains constant while it shrinks but the electrical stress changes with surface area. At a certain point the Rayleigh limit is reached where the droplet can no longer withstand the increasing charge density due to the balance between electric stress and surface tension. At this point, the droplets undergo Coulomb fission into smaller offspring droplets which then continue to shrink [36,37].

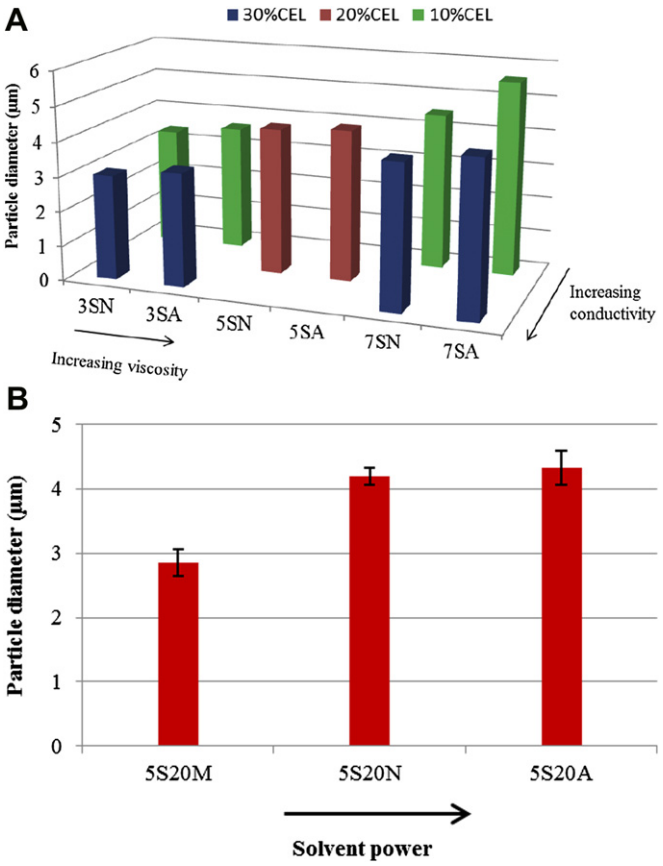

Fig. 3. Mean diameter of particles produced at different solute concentration and drug loading (A), and particles prepared at 5% solute concentration using different solvents (B). Error bars indicate standard deviation from the mean. $n > 200$ particles.

3. The solutes in the droplet diffuse towards the core of the droplet as solvent evaporates at the surface. However, the increasing solute concentration in the droplets eventually results in the solute components beginning to deposit and cover the entire surface forming a shell, and from this point onwards the droplet diameter remains constant [23,38].
4. Solvent evaporation continues but takes place from inside the shell until the particle is dry. Depending on the solute concentration in the droplets as well as the balance between evaporation rate and polymer diffusion rate and conformation, different shell thicknesses will form [25,37,39]).

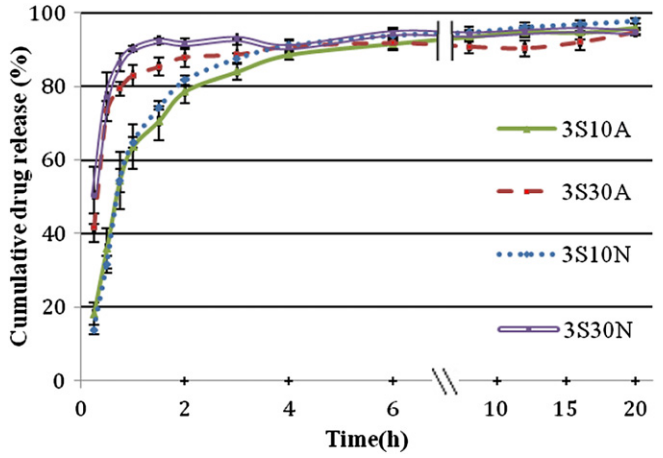

Fig. 4. Drug release profile of microparticles prepared with 3% solute concentration and different drug loading in ACE or ACN, measured over 20 h, $n = 3–5$.

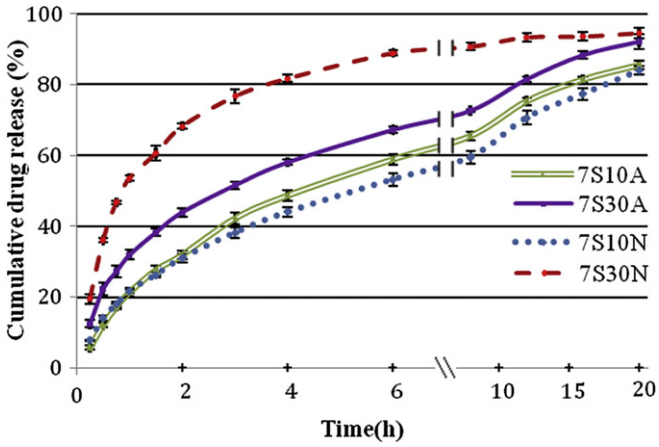

Fig. 5. Drug release profile of microparticles prepared with 7% solute concentration and different drug loading in ACE or ACN, measured over 20 h, $n = 3–5$.

It is believed that solvent evaporation and polymer diffusion are the two main mechanisms determining both particle formation and their resulting properties [24]. Polymer diffusion refers to the mechanism by which polymer molecules migrate away from the surface due to the concentration gradient resulting from accumulation of polymer at the surface. The solvent evaporation rate determines how quickly the droplets begin to solidify. Evaporation of solvent from a droplet is a coupled heat and mass transport that is driven by the difference between the vapor pressure of the solvents and their partial pressure in the gas phase. The rate at which this process takes place is controlled by the balance of energy required to vaporize the solvent and the energy transported to the surface of the droplet [11]. The evaporation mechanism of droplets containing dissolved solids is different from that of pure solvents and takes place via the different stages of evaporation explained above. The evaporation rate from a droplet depends on the initial diameter of the droplet and increases with the decrease in its squared diameter. Also, a more volatile liquid will have a faster evaporation rate and results in more rapid particle drying. In this context, a fast evaporation of the solvent is generally believed to result in porous or hollow particles but coupled with fast polymer

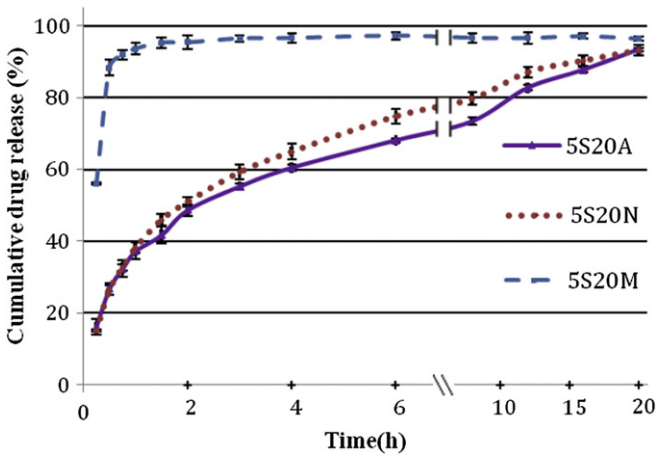

Fig. 6. Drug release profile of microparticles prepared with 5% solute concentration and 20% drug loading in ACE, ACN or ACE:MeOH, measured over 20 h, $n = 3–5$.

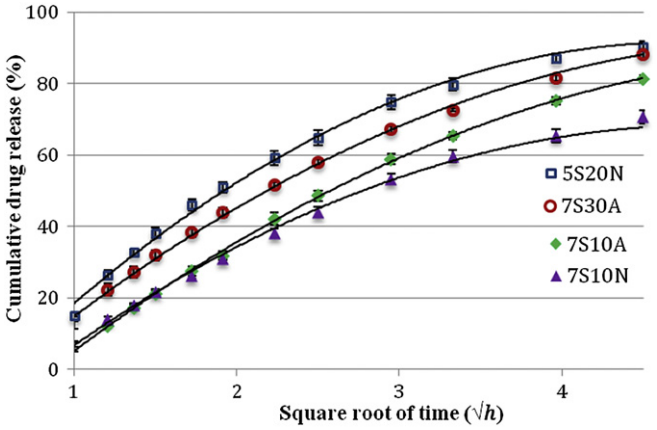

Fig. 7. Selected drug release curves fitted to the modified Higuchi model.

diffusion inside the droplets dense, solid particles can be formed [23,40,41].

When more than one solute constituent is added in the spraying solution the diffusion mechanism of each constituent during evaporation can be different depending on the properties of these constituents [42]. The understanding of such diffusion processes seems to be limited currently but it is hypothesized that the diffusion of different components in a droplet can happen in a non-equilibrated fashion, leading to phase separation among the different constituents [43,44]. Such phase separation between solutes would be of interest as it can provide a useful route for controlling the distribution of material within the final particles. The diffusion process and particle formation in general may further be influenced by the electric field surrounding the droplet and the electric charge of the droplet. It has been shown that the evaporation rate of solvents increases when an electric field is applied and that an AC field has more impact on the heat transfer than does a DC field [45,46]. Such enhanced heat transfer may be of significance when small droplets are exposed to a strong electric field, influencing the otherwise passive drying process.

4.2. Effect of the solvents on the morphology of the microparticles

It is known from studies using electrospraying but also from other atomization techniques that the properties of the solution affect both particle size and morphology in many ways. In similar studies it was observed that particle morphology may depend on solute concentration and on drug loading. With low solute concentration it has been observed that spherical particles could not form and that particles tended to collapse or shrink to give a "raisin-like" morphology [47]. For electrospraying it has been observed that with high solute concentration, at a point where polymer entanglement begins before coulomb fission of droplets, elongated particles were formed [23]. It has further been observed that particles tended to be more spherical and less concave as the polymer concentration was increased towards the maximum value at which a stable jet could be achieved [25]. These findings correlate well with the observations made from Fig. 2 where particles with both raisin-like appearance and collapsed particles were obtained at low concentration, whereas higher concentration gave rise to spherical particles but although not elongated particles. The differences observed in particle morphology on Fig. 2 are partly explained by the overlap concentration of PLGA in the different solvents (Table 3). In Table 4 it is seen that that the solutions of samples 3S10A, 3S30A, 3S10N, 3S30N, 5S20N and 5S20M all have a PLGA concentration below the overlap concentration indicating that polymer entanglement has not yet been initiated. The particles formed from these solutions are slower at reaching polymer entanglement and thus do not manage to get a smooth morphology as the particles prepared at PLGA concentrations above the overlap concentration. This makes sense when observing the SEM images of the particles in which those prepared at PLGA concentrations below the overlap concentration result in collapsed, porous, aggregated or "raisin-like" particles. The differences in morphology seen between particles prepared using ACE and ACN at low concentration can also be explained by the higher solubility of PLGA in ACE (higher intrinsic viscosity, see Table 3) and hence a greater ability to retain the particle shell through polymer diffusion during drying. They thereby manage to avoid collapsing and instead shrink. Xie et al observed in a similar study using electrospraying that a faster evaporation rate of the droplets resulted in a smoother particle surface [18].

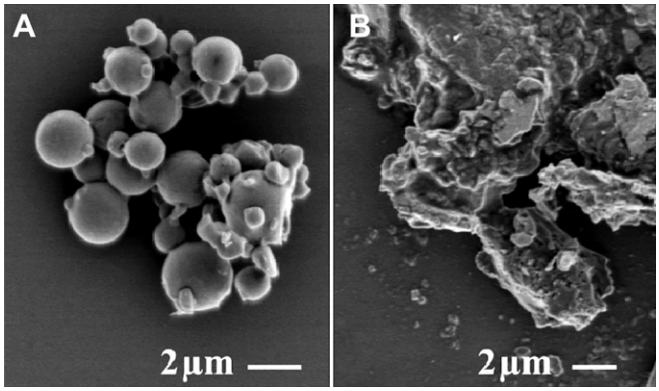

Fig. 8. SEM images of particles from sample 5S20A (A) and 5S20M (B) after drug release.

When comparing the particles formed using either ACE or ACN one could expect to observe a difference based on the difference in evaporation rate of the solvents. Although particles prepared with ACN at high solute concentrations seem more prone to form pores on the surface a clear trend was not found at low solute concentrations. The collapse of particles from sample 3S30N, however, indicates that slower evaporation of ACN could have resulted in the solvent not fully managing to evaporate before the particles were being collected. The impact of the particle at collection may have resulted in its collapse because the shell was not thick enough. The grainy morphology of the particles in sample 5S20M is explained by the effect of MeOH on the solubility of PLGA in the solution. With the intrinsic viscosity of PLGA in ACE:MeOH being significantly lower than for the two other solvents it is likely that the polymer chains are more curled up and take up less volume [34]. These compact chains could also have resulted in faster polymer diffusion during solvent evaporation. It is believed that the small grains observed via the SEM start forming due to the coiled up state of the polymer and then aggregate as the solvent evaporate.

4.3. Effect of the solvents on the size of the microparticles produced

The summary of particle mean diameters in Fig. 3 shows that the solute concentration, drug loading and the type of solvent used all influence the particle size. Several studies have demonstrated that an increase in solute concentration and hence viscosity results in larger particles [48]. The drug loading mainly influences polymer concentration and hence solution viscosity but also has a significant effect on the electrical conductivity of the solution as seen in Table 2. An increase in conductivity reduces the particle size by increasing the tendency for the droplets to undergo coulomb fission [49]. The influence on the particle size caused by the solvent

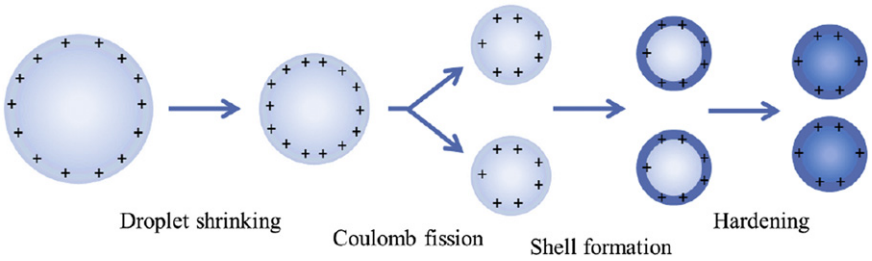

Fig. 9. Schematic diagram of general phases in the particle formation process with electrospraying.

appears to mainly be driven by the differences in electrical conductivity. The viscosities of the solvents are similar and if anything they show contradictory effects. Also, the slower evaporation of ACN (Table 1) could have resulted in more pronounced droplet shrinking and was further enhanced by the lower solvent power of ACN (Table 3) and hence increased polymer diffusion. The conductivity of ACE is the lowest of the three solvents used and therefore results in the largest particles. The conductivity of ACN is slightly higher and this could therefore explain the slightly smaller particles obtained. ACE:MeOH has a higher electrical conductivity than ACE and ACN and was seen to give smaller particles than the other solvents. Similar effects of type of solvent on the particle size were observed by Xie et al. [18]. The effect of solvent evaporation rate on particle size can only be speculated upon in this work as information on particle density is necessary to assess whether more porous particles were produced with ACN due to the balance between polymer diffusion and solvent evaporation.

4.4. Effect of solvents on the release behavior of microparticles

Typically, it is desirable to have a controlled release of the drug from the microparticles. In some cases it is suitable to have a sustained release over a long period and in other cases it is preferable to have a constant release rate over a short period or even instantaneous release (i.e. burst release). Figs. 4–6 show that in this study the particles released most of their payload within 20 h and for some particles release occurred much more quickly. Some "burst" release seems to take place from the surface of all samples, judging from the quick release observed in the beginning. Generally, high drug loading gave more burst compared with low drug loading and decreasing solute concentration resulted in more burst effect. This indicates that the particles with high burst effect had a higher drug concentration close to the particle surface or had a larger surface to volume ratio as a result of their smaller size or higher porosity. The remaining drug release seems to be diffusion dependent and the curves follow the same trend as for the burst release, with high burst samples continuing with a fast release.

Curve fitting for the selected microparticles with slow release (see Fig. 7) supports the hypothesis of a diffusion driven release mechanism according to a modified Higuchi release model. The Higuchi model is based under the assumptions that the drug molecules are homogeneously dispersed within the polymer matrix and are released through diffusion from the particle surface mediated by the surrounding medium [31]. However, the Higuchi model was modified by using a level 2 polynomial regression due to a much improved correlation over a straight line. The rate of diffusion was observed to fall off with time compared with a conventional Higuchi model possibly for two reasons (1) a reduced rate of diffusion due to distance traveled and (2) a possible lack of sink condition. Moreover, not all release profiles for the samples studied fit well with the Higuchi model, in particular those with quicker release rates. This indicates that either these particles contained a high degree of porosity or the drug was unevenly distributed towards the surface of the particles resulting in a lower diffusion barrier provided by the polymer matrix. Studies by other researchers on the drug release from biodegradable microparticles prepared with electrospraying and other preparation techniques such as spray drying show similar trends in the release profile with an initial burst followed by a diffusion-mediated release [10,19,43]. However, in many of these studies the release took place over a much longer time span of several days to weeks, thus including release via polymer erosion, although the particles were of similar size. The quicker release observed in the present study can be explained partly due to porosity of the particles and the small molecular size of the drug (M_w=381.38 g/mol) both of which have been shown to increase mobility and enable quicker release [4,7,50].

The full release mechanism is complex but in the case of diffusion driven release it is believed to mainly depend on particle size and porosity [7,48]. Size dependent release was also seen here where the largest particles (sample 7S10A and 7S10N) had the slowest release and the smallest particles had the quickest release due to their respective surface to volume ratios. An increase in drug loading results in more rapid release and this is believed to be partly due to their smaller size but also because of the smaller amount of polymer acting as a diffusional barrier from drug release as explained by Pinon Segundo et al. [51]. Comparisons of drug release from samples prepared using ACE and ACN show that those prepared in ACN release slightly more quickly than those prepared in ACE, except for samples 7S10A and 7S10N. This is believed to be partly related again to the particle size where those prepared in ACN are slightly smaller and therefore release more quickly. Also, from the SEM images in Fig. 2 it seems that the particles prepared using ACN are slightly more porous on their surfaces. These particles could also be more porous inside (see Fig. 2D) due to less intra-polymer entanglements compared with ACE, giving a less homogenous network of the polymer. Even a slightly higher porosity would have a visible effect on the drug release rate from the particles given the larger surface area. Internal porosity would act as channels to allow more rapid penetration of the dissolution medium into the core and thus faster solubilization. Further, particles that are collapsed (Fig. 2D) expose more surface and should thereby also have quicker release. Also, ACN being a poorer solvent means that the polymer is more packed and perhaps cannot incorporate as much drug within the matrix. Why the faster release of particles prepared with ACN is more prominent at 30% drug loading, however, cannot be fully explained from the information available. It could be due to differences in the polymer and drug concentration gradients of particles prepared in ACE and ACN or the better ability of particles prepared in ACE to incorporate the drug in the matrix at high drug loading.

The drug release from particles prepared in ACE:MeOH (sample 5S20M) was much faster compared with that from samples 5S20A and 5S20N and can be explained in terms of the observed

morphology. The particles in sample 5S20M appear to be composed from the assembly of small grains and therefore could be expected to disintegrate when placed in the release medium, greatly increasing the surface area-to-volume ratio resulting in instantaneous release of the drug. This idea of disintegration is supported by the images on Fig. 8 showing loss of particle structure after releasing their drug, most likely related to the compact conformation of PLGA in the poor solvent. Such disintegration and instantaneous release from an otherwise stable particle could be of interest for formulations in which the drug needs to be released at a specific site.

5. Conclusions

In the present study CEL-loaded PLGA microparticles were prepared via electrospraying using different solvents and polymer concentrations to investigate their influence upon particle formation, morphology and drug release. The solvents ACE and ACN as well as a binary solvent of ACE and MeOH with a molar ratio of 75:25 were selected to study the influence of solvent power, evaporation rate and electrical conductivity on the resulting particle properties. With all solvents particles between 2 and 7 μm were produced with a relatively narrow size distribution (polydispersivity index of 6–16%). Drug release studies showed that the release could be controlled to take place in a time span of 1–20 h with varying levels of burst release. Particles with different morphologies were obtained depending on the different processing conditions where those prepared at low solute concentration showed the most distinct differences. ACE solutions had high solvent power and low electrical conductivity and resulted in the largest particles with raisin-like morphology at low solute concentration. The release rate from particles prepared in ACE was slower than for particles prepared in other solvents. Solutions with ACN had lower evaporation rates and solvent power than ACE but slightly higher conductivity and resulted in slightly smaller particles with collapse occurring at low polymer concentration. The release rates from these particles were slightly faster than for those prepared in ACE. The ACE/MeOH solute solution had the lowest solvent power and the highest conductivity and resulted in the smallest particles with small grainy features ($\sim$100 nm) indicating early precipitation of PLGA before shell formation. Drug release from these particles took place almost instantaneously indicating disintegration of the particles. The presence of a poor solvent, MeOH, had a significant role in the particle formation as well as particle morphology and drug release and will be further investigated. Overall, the results in this study support the use of electrospraying as a means of producing microparticles designed for optimum drug delivery.

Acknowledgements

The authors would like to thank the Danish Agency for Science, Technology and Innovation and Veloxis Pharmaceuticals A/S for financial support of this project.

References

[1] Tran VT, Benoit JP, Venier-Julienne MC. Why and how to prepare biodegradable, monodispersed, polymeric microparticles in the field of pharmacy? International Journal of Pharmaceutics 2011 Apr 4;407(1–2):1–11.
[2] Kim KK, Pack DW. In: Ferrari M, Lee AP, Lee LJ, editors. Microspheres for drug delivery BioMEMS and biomedical nanotechnology. US: Springer; 2006. p. 19–50.
[3] Varde NK, Pack DW. Microspheres for controlled release drug delivery. Expert Opinion on Biological Therapy 2004 Jan 1;4(1):35–51.
[4] Freiberg S, Zhu XX. Polymer microspheres for controlled drug release. International Journal of Pharmaceutics 2004 Sep 10;282(1–2):1–18.
[5] Klose D, Siepmann F, Elkharraz K, Siepmann J. PLGA-based drug delivery systems: importance of the type of drug and device geometry. International Journal of Pharmaceutics 2008 Apr 16;354(1–2):95–103.
[6] Edlund U, Albertsson A. Degradable polymer microspheres for controlled drug delivery, Degradable aliphatic polyesters. 157 ed. Berlin/Heidelberg: Springer; 2002. p. 67–112.
[7] Klose D, Siepmann F, Elkharraz K, Krenzlin S, Siepmann J. How porosity and size affect the drug release mechanisms from PLGA-based microparticles. International Journal of Pharmaceutics 2006 May 18;314(2):198–206.
[8] Rosca ID, Watari F, Uo M. Microparticle formation and its mechanism in single and double emulsion solvent evaporation. Journal of Controlled Release 2004 Sep 30;99(2):271–80.
[9] Tamber H, Johansen P, Merkle HP, Gander B. Formulation aspects of biodegradable polymeric microspheres for antigen delivery. Advanced Drug Delivery Reviews 2005 Jan 10;57(3):357–76.
[10] Mu L, Feng SS. Fabrication, characterization and in vitro release of paclitaxel (taxol) loaded poly (lactic-co-glycolic acid) microspheres prepared by spray drying technique with lipid/cholesterol emulsifiers. Journal of Controlled Release 2001 Oct 19;76(3):239–54.
[11] Vehring R. Pharmaceutical particle engineering via spray drying. Pharmaceutical Research 2008 May;25(5):999–1022.
[12] Bittner B, Mäder K, Kroll C, Borchert HH, Kissel T. Tetracycline-HCl-loaded poly(DL-lactide-co-glycolide) microspheres prepared by a spray drying technique: influence of γ-irradiation on radical formation and polymer degradation. Journal of Controlled Release 1999 May 1;59(1):23–32.
[13] Valo H, Peltonen L, Vehvilainen S, Karjalainen M, Kostiainen R, Laaksonen T, et al. Electrospray encapsulation of hydrophilic and hydrophobic drugs in poly(L-lactic acid) nanoparticles. Small 2009 Aug 3;5(15):1791–8.
[14] Ding L, Lee T, Wang CH. Fabrication of monodispersed taxol-loaded particles using electrohydrodynamic atomization. Journal of Controlled Release 2005 Feb 2;102(2):395–413.
[15] Champion JA, Mitragotri S. Role of target geometry in phagocytosis. Proceedings of the National Academy of Sciences of the United States of America 2006 Mar 28;103(13):4930–4.
[16] Champion JA, Katare YK, Mitragotri S. Particle shape: a new design parameter for micro- and nanoscale drug delivery carriers. Journal of Controlled Release 2007 Aug 16;121(1–2):3–9.
[17] Costa P, Sousa Lobo JM. Modeling and comparison of dissolution profiles. European Journal of Pharmaceutical Sciences 2001 May;13(2):123–33.
[18] Xie J, Marijnissen JC, Wang CH. Microparticles developed by electrohydrodynamic atomization for the local delivery of anticancer drug to treat C6 glioma in vitro. Biomaterials 2006 Jun;27(17):3321–32.
[19] Xu Y, Hanna MA. Electrospray encapsulation of water-soluble protein with polylactide. Effects of formulations on morphology, encapsulation efficiency and release profile of particles. International Journal of Pharmaceutics 2006 Aug 31;320(1–2):30–6.
[20] Enayati M, Ahmad Z, Stride E, Edirisinghe M. Preparation of polymeric carriers for drug delivery with different shape and size using an electric jet. Current Pharmaceutical Biotechnology 2009;10(6):600–8. Ref Type: Abstract.
[21] Jaworek A, Sobczyk AT. Electrospraying route to nanotechnology: an overview. Journal of Electrostatics 2008 Mar;66(3–4):197–219.
[22] Bock N, Woodruff MA, Hutmacher DW, Dargaville TR. Electrospraying a reproducible method for production of polymeric microspheres for biomedical applications. Polymers 2011;3(1):131–49. Ref Type: Journal (Full).
[23] Almería B, Deng W, Fahmy TM, Gomez A. Controlling the morphology of electrospray-generated PLGA microparticles for drug delivery. Journal of Colloid and Interface Science 2010 Mar 1;343(1):125–33.
[24] Yao J, Kuang Lim L, Xie J, Hua J, Wang CH. Characterization of electrospraying process for polymeric particle fabrication. Journal of Aerosol Science 2008 Nov;39(11):987–1002.
[25] Xue L, Mao L, Cai Q, Yang X, Jin R. Preparation of amino acid ester substituted polyphosphazene microparticles via electrohydrodynamic atomization. Polymers for Advanced Technologies 2011 [n/a].
[26] Chawla G, Gupta P, Thilagavathi R, Chakraborti AK, Bansal AK. Characterization of solid-state forms of celecoxib. European Journal of Pharmaceutical Science 2003 Nov;20(3):305–17.
[27] Smallwood IM. Handbook of organic solvent properties. Arnold; 1996.
[28] Jen Tsi Y. The viscosity of macromolecules in relation to molecular conformation. In: Anfinsen CB, editor. Advances in protein chemistry, vol. 16. Academic Press; 1962. p. 323–400.
[29] Son WK, Youk JH, Lee TS, Park WH. The effects of solution properties and polyelectrolyte on electrospinning of ultrafine poly(ethylene oxide) fibers. Polymer 2004 Apr;45(9):2959–66.
[30] Baldursdottir SG, Kjøniksen AL, Karlsen J, Nyström B, Roots J, Tønnesen HH. Riboflavin-photosensitized changes in aqueous solutions of alginate. Rheological studies. Biomacromolecules 2003 Feb 1;4(2):429–36.
[31] Higuchi T. Mechanism of sustained-action medication. Theoretical analysis of rate of release of solid drugs dispersed in solid matrices. Journal of Pharmaceutical Science 1963;52(12):1145–9.
[32] Ganan-Calvo AM, Davila J, Barrero A. Current and droplet size in the electrospraying of liquids. Scaling laws. Journal of Aerosol Science 1997;28(2):249–75.
[33] Jayasinghe SN, Edirisinghe MJ. Effect of viscosity on the size of relics produced by electrostatic atomization. Journal of Aerosol Science 2002;33(10):1379–88.
[34] Debye P, Bueche AM. Intrinsic viscosity, diffusion, and sedimentation rate of polymers in solution. The Journal of Chemical Physics 1948 Jun;16(6):573–9.

[35] Günther R. Combustion and mass transfer. Von D.B. Spalding. In: Combustion and mass transfer. Oxford, New York: Pergamon Press; 1979. Chemie Ingenieur Technik 1979;52(2):83–263.
[36] Smith JN, Flagan RC, Beauchamp JL. Droplet evaporation and discharge dynamics in electrospray ionization. Journal of Physical Chemistry A 2002 Aug 24;106(42):9957–67.
[37] Rayleigh L. On the equilibrium of liquid conducting masses charged with electricity. Philosophical Magazine; 1882:184.
[38] Okuzono T, Ozawa K, Doi M. A simple model of skin formation caused by solvent evaporation in polymer solutions. Physics Review Letters; 2006:97.
[39] Masters K. Spray drying in practice. 3rd ed. SprayDryConsult International; 2002.
[40] Geankoplis CJ. Transport processes and unit operations. 3rd ed. Prentice Hall; 1993.
[41] Maa YF, Costantino HR, Nguyen PA, Hsu CC. The effect of operating and formulation variables on the morphology of spray-dried protein particles. Pharmaceutical Development and Technology 1997 Jan 1;2(3):213–23.
[42] Grassmann P, Widmer F, Sinn H. Einführung in die thermische Verfahrenstechnik. 3rd ed. Gruyter; 1996.
[43] Wang FJ, Wang CH. Sustained release of etanidazole from spray dried microspheres prepared by non-halogenated solvents. Journal of Controlled Release 2002 Jun 17;81(3):263–80.
[44] Luo CJ, Nangrejo M, Edirisinghe M. A novel method of selecting solvents for polymer electrospinning. Polymer 2010 Mar 24;51(7):1654–62.
[45] Liu Y, Li R, Wang F, Yu H. The effect of electrode polarity on EHD enhancement of boiling heat transfer in a vertical tube. Experimental Thermal and Fluid Science 2005 Jun;29(5):601–8.
[46] Zheng DJ, Liu HJ, Cheng YQ, Li LT. Electrode configuration and polarity effects on water evaporation enhancement. International Journal of Food Engineering 2011;7(2). Article 12.
[47] Bittner B, Kissel T. Ultrasonic atomization for spray drying: a versatile technique for the preparation of protein loaded biodegradable microspheres. Journal of Microencapsulation 1999 Jan 1;16(3):325–41.
[48] Berkland C, King M, Cox A, Kim K, Pack DW. Precise control of PLG microsphere size provides enhanced control of drug release rate. Journal of Controlled Release 2002 Jul 18;82(1):137–47.
[49] Hartman RPA, Brunner DJ, Camelot DMA, Marijnissen JCM, Scarlett B. Electrohydrodynamic atomization in the cone-jet mode physical modeling of the liquid cone and jet. Journal of Aerosol Science 1999 Aug;30(7):823–49.
[50] Huang X, Brazel CS. On the importance and mechanisms of burst release in matrix-controlled drug delivery systems. Journal of Controlled Release 2001 Jun 15;73(2–3):121–36.
[51] Pinon-Segundo E, Ganem-Quintanar A, Alonso-Perez V, Quintanar-Guerrero D. Preparation and characterization of triclosan nanoparticles for periodontal treatment. International Journal of Pharmaceutics 2005 Apr 27;294(1–2):217–32.